Frontiers in Bioscience Landmark

Front. Biosci. (Landmark Ed) **2026**; 31(4): 48054
https://doi.org/10.31083/FBL48054

Original Research

NDRG2 Drives DRP1 Phosphorylation to Promote the Progression of Pulmonary Hypertension

Jiayong Luo[1,†], Jinyu Chang[2,†], Yi Liu[1,2,3], Yusang Shao[1], Yanyan Zhang[1], Yingru Zheng[2], Enfang Xiao[2], Yanqing Xie[1], Shuangshuang Tu[1], Haoxuan Lu[1], Wenming He[1,3,*]

[1]Department of Cardiology, The First Affiliated Hospital of Ningbo University, 315010 Ningbo, Zhejiang, China
[2]Department of Respiratory Disease, The First Affiliated Hospital, Jinzhou Medical University, 121000 Jinzhou, Liaoning, China
[3]Institute of One Health Science, School of Civil & Environmental Engineering and Geography Science, State Key Laboratory for Quality and Safety of Agro-products, Ningbo University, 315211 Ningbo, Zhejiang, China
*Correspondence: fyhewenming@nbu.edu.cn (Wenming He)
[†]These authors contributed equally.

Academic Editor: Esteban C. Gabazza
Submitted: 7 November 2025 Revised: 26 January 2026 Accepted: 5 February 2026 Published: 14 April 2026

Abstract

Background: Pulmonary hypertension (PH) is a progressive disease characterized by obstructive pulmonary vascular remodeling, for which no curative therapies effectively reverse disease progression. This study investigated whether N-myc downstream-regulated gene 2 (*NDRG2*) drives PH pathogenesis by regulating mitochondrial dynamics. **Methods**: *NDRG2* expression was examined in two rat models of PH (SuHx and MCT). Functional studies using *NDRG2* knockdown and overexpression in PASMCs assessed phenotypic switching, proliferation, migration, mitochondrial morphology, and bioenergetics. The *NDRG2-DRP1* interaction was investigated via co-immunoprecipitation and immunofluorescence. An in vivo rescue experiment was performed using intratracheal AAV9-shNDRG2 delivery in SuHx rats. **Results**: *NDRG2* was significantly upregulated in PASMCs from PH rats, hypoxic human PASMCs, and patients with PH. *NDRG2* knockdown attenuated, while its overexpression exacerbated, hypoxia-induced phenotypic switching, proliferation, and migration of PASMCs. Mechanistically, NDRG2 directly interacted with DRP1 and specifically promoted its activating phosphorylation at Ser616, leading to excessive mitochondrial fission, ATP depletion, and oxidative stress. These pathogenic effects were abolished by concurrent *DRP1* knockdown. *In vivo*, *NDRG2* knockdown ameliorated hemodynamic indices, right ventricular hypertrophy, pulmonary vascular remodeling, and exercise capacity in SuHx rats. **Conclusions**: NDRG2 drives PH progression by promoting DRP1-mediated mitochondrial fission and vascular remodeling. The NDRG2-DRP1 axis represents a candidate pathway for therapeutic exploration in PH.

Keywords: NDRG2 protein; dynamin-related protein 1; hypertension; pulmonary; mitochondrial dynamics; genetic vectors; vascular remodeling

1. Introduction

Pulmonary hypertension (PH) is a life-threatening pulmonary vascular disorder characterized by pathological pulmonary vascular remodeling and lumen obstruction, leading to a persistent increase in pulmonary vascular resistance and ultimately resulting in right-sided heart failure [1–3]. Although current therapies (e.g., endothelin receptor antagonists and prostacyclin analogues) can partially alleviate vasoconstriction, they generally fail to effectively halt or reverse structural vascular remodeling [4–6]. Therefore, exploring novel targets capable of directly reversing vascular remodeling is of great importance.

Excessive proliferation, migration, and phenotypic switching of pulmonary arterial smooth muscle cells (PASMCs) from a contractile to a synthetic secretory phenotype are considered central cellular mechanisms driving pulmonary vascular remodeling and lumen occlusion [7].

N-myc downstream-regulated gene 2 (NDRG2) is a member of the N-myc downstream-regulated gene family, which possesses an α/β hydrolase domain and has been demonstrated to be widely involved in regulating key processes such as stress responses, cell proliferation, and migration [8,9]. NDRG2 expression is upregulated under various stress conditions, including hypoxia and cerebral ischemia, yet its expression pattern exhibits significant cell-type specificity. For instance, hypoxia promotes NDRG2 expression via direct binding of HIF-1α to its promoter in A549 cells [10], whereas hypoxia-induced miR-346 exerts an inhibitory effect in cells such as OS-RC-2 [11]. Our previous study established a crucial role for NDRG1 in promoting pulmonary vascular remodeling in PH [12]. Given the high homology between NDRG2 and NDRG1, we hypothesize that NDRG2 may play a similar role. Furthermore, supporting this notion, NDRG2 has been reported to participate in the progression of various cardiovascular dis-

eases, such as cardiac remodeling in models of myocardial ischemia–reperfusion injury [13,14] and heart failure [15]. However, despite these suggestive associations, the specific role and mechanism of NDRG2 in PH remain unknown.

On the contrary, aberrant mitochondrial fragmentation has been identified as a significant contributor to PH, exacerbating vascular remodeling by promoting the proliferation, migration, and phenotypic switching of PASMCs, whereas the inhibition of this process confers therapeutic benefits [16–18]. This pathological mitochondrial fission event is primarily regulated by the post-translational modifications of dynamin-related protein 1 (DRP1): phosphorylation of DRP1 at serine 616 (Ser616) promotes its translocation to mitochondria and initiates fission, whereas the phosphorylation at serine 637 (Ser637) exerts an inhibitory effect [16,19]. Given the central role of NDRG2 in regulating cellular signaling pathways, we hypothesize that NDRG2 may influence mitochondrial dynamics, and thereby contribute to PH progression, by perturbing the balance of DRP1 phosphorylation.

Based on this background, this study was conducted to systematically address three core questions: (1) to determine whether NDRG2 is involved in the pathogenesis and progression of PH; (2) to investigate the molecular mechanism by which NDRG2 promotes vascular remodeling, specifically examining whether it acts by regulating DRP1 phosphorylation-mediated mitochondrial fragmentation; and (3) to evaluate the potential therapeutic value of targeting NDRG2 for ameliorating pathological vascular remodeling.

2. Materials and Methods

2.1 Animal Studies

All experimental procedures involving animals were approved by the Animal Ethics Committee of Ningbo University (Approval No.: AEWC-NBU20250371). Twenty-four male Sprague–Dawley (SD) rats (aged 6–8 weeks and weighing 180–220 g) were housed under standard laboratory conditions and randomly allocated to four experimental groups (n = 6 per group): normoxia control, normoxia + AAV9-shNDRG2, hypoxia + Sugen 5416 (SuHx), and SuHx + AAV9-shNDRG2. For genetic knockdown, the rats received an intratracheal instillation of adeno-associated virus 9 (AAV9) encoding short hairpin RNA against NDRG2 (AAV9-shNDRG2; 1.75×10^{13} viral genomes/mL; GeneChem, Shanghai, China) under isoflurane (3%) anesthesia. Briefly, a soft catheter was inserted into the trachea, and 25 µL of the viral suspension was administered [20]. The rats were maintained in an upright position for 1 min post-instillation to facilitate lung distribution and allowed a 2-week recovery for viral expression.

The PH model was subsequently induced. The rats in the SuHx and SuHx+AAV9-shNDRG2 groups were housed in a hypoxic chamber (10% O_2, Oxycycler A84XOV; BioSpherix, Parish, NY, USA), with CO_2 maintained below 3% using soda lime. On the first day of hypoxia, these rats received a single intraperitoneal injection of Sugen 5416 (20 mg/kg; Bio-Techne, America) dissolved in vehicle. The rats in the control groups were maintained under normoxia (21% O_2) throughout the experiment. The body weight and health status were monitored weekly. At the study endpoint, all rats were euthanized under sodium pentobarbital anesthesia (150 mg/kg, i.p.).

The exercise capacity was evaluated using a motorized treadmill. After acclimatization, the test commenced at 10 m/min, with speed increasing by 5 m/min every 5 min until exhaustion or a maximum of 30 min. The total running distance was recorded [21].

Following euthanasia, the heart and lung tissues were harvested. The right ventricle (RV) was dissected and weighed separately from the left ventricle plus septum (LV + S) to calculate the RV hypertrophy index (RVHI = RV/[LV + S]). The right lung was snap-frozen for molecular analysis. The left lung was inflation-fixed with 4% paraformaldehyde (PFA, P0099-3L, Beyotime, Shanghai, China), processed for paraffin embedding, and sectioned (5 µm). Hematoxylin and eosin (H&E)-stained sections were used to quantify the wall thickness (%) of pulmonary arterioles in vessels with an external diameter of 50–150 µm, calculated as (medial wall thickness/external diameter) × 100. After acclimatization, the rats were randomly allocated to experimental groups using a computer-generated random number sequence. Investigators performing hemodynamic measurements and all quantitative histological and morphological analyses were blinded to the group identity of the animals and samples. Personnel responsible for animal treatment, virus delivery, and tissue collection were not blinded due to the nature of the procedures.

2.2 Hemodynamic Assessment

RV hemodynamics were assessed via direct catheterization before euthanasia. Under anesthesia (sodium pentobarbital, 40 mg/kg, i.p.), the right external jugular vein was cannulated with a heparinized PE-50 catheter (Taimeng, Chengdu, China). The catheter was advanced into the RV under continuous-pressure monitoring (BL-420N; Taimeng, Chengdu, China). RV systolic pressure (RVSP) was recorded in real time and used as a surrogate for pulmonary arterial systolic pressure.

2.3 Histopathological Examination

For immunofluorescence analysis, 5-µm lung sections were deparaffinized, rehydrated, and subjected to antigen retrieval. The sections were blocked with 5% bovine serum albumin (BSA) and incubated overnight at 4 °C with primary antibodies against α-smooth muscle actin (α-SMA) or NDRG2 (1:150, ab174850; Abcam, Cambridge, UK). After washing, the sections were incubated with Alexa Fluor 488–conjugated secondary antibodies (1:500; Invitrogen, Carlsbad, CA, USA). The nuclei were counterstained with

Table 1. Antibodies for western blot analysis.

Antibody	Cat. No.	Producer	Dilution ratio
Anti-NDRG2	Ab174850	Abcam	1:1000
Anti-DRP1	Ab184247	Abcam	1:2000
Anti-p-DRP1 (Ser616)	Ab614755	Abcam	1:2000
Anti-p-DRP1 (Ser637)	Ab193216	Abcam	1:2000
Anti-MFN1	Ab221661	Abcam	1:2000
Anti-MFN2	Ab124773	Abcam	1:1000
Anti-OPA1	Ab157457	Abcam	1:1000
Anti-FN1	Ab45688	Abcam	1:1000
Anti-Col I	Ab6308	Abcam	1:2000
Anti-α-SMA	#19245	CST	1:5000
Anti-β-actin	AF7018	Affinity	1:5000

4′,6-diamidino-2-phenylindole (DAPI). The images were acquired using a fluorescence microscope (DM1000; Leica, Wetzlar, Germany). At least six biological replicates per group were analyzed.

2.4 Cell Culture and Treatments

Human pulmonary arterial smooth muscle cells (HPASMCs; #3110, Sciencell, Carlsbad, CA, USA) were cultured in smooth muscle cell medium (#1101; ScienCell) at 37 °C with 5% CO_2. Following is the example of the statement for cell lines: All cell lines were validated by STR profiling and tested negative for mycoplasma. Experiments used cells at passages 2–6. For stable NDRG2 knockdown, the cells were transduced with lentiviral vectors encoding short hairpin RNA (shRNA) against NDRG2 (shNDRG2; GeneChem). The targeting sequence was as follows: 5′-CCGGGAGGACATGCAGGAAATCATTCTCGAGAATGATTTCCTGCATGTCCTCTTTTTG-3′. A nontargeting shRNA (shRandom) served as the control. The cells were infected at a multiplicity of infection of 20 in the presence of 8 µg/mL polybrene for 24 h, followed by selection with 2 µg/mL puromycin for 72 h. For hypoxia treatment, the transduced cells were exposed to 1% O_2 in a tri-gas incubator for 24 h. This condition was selected based on previous study showing that it robustly induced PASMC dysfunction [22].

2.5 Immunofluorescence Staining

The fixed and permeabilized HPASMCs were blocked with 5% BSA (ST023-50g, Beyotime, Shanghai, China) and incubated with primary antibodies against the translocase of outer membrane 20 (TOMM20; 1:200; ab186735, Abcam) or co-incubated with anti-NDRG2 and anti-dynamin-related protein 1 (DRP1; 1:200; ab184247, Abcam) antibodies. After incubation with fluorophore-conjugated secondary antibodies, the nuclei were stained with DAPI. The confocal images were captured using a Zeiss LSM 880 microscope (Carl Zeiss AG, Oberkochen, Germany). Specificity was confirmed using isotype and secondary antibody–only controls.

2.6 Cell Proliferation and Migration Assays

Cell proliferation was assessed using 5-ethynyl-2′-deoxyuridine (EdU) incorporation and cell counting kit-8 (CCK-8) assays. For the EdU assay, the cells were pulsed with 10 µM EdU for 2 h, fixed, and detected using a Click-iT kit (K1076l; APExbio, Houston, TX, USA). EdU-positive nuclei were counted. For the CCK-8 assay, the cells were seeded in 96-well plates, and the absorbance at 450 nm was measured 2 h after adding CCK-8 reagent at the indicated time points.

Cell migration was evaluated using Transwell chambers. HPASMCs (1×10^4) in serum-free medium were placed in the upper chamber, with 10% fetal bovine serum as a chemoattractant placed in the lower chamber. After 24 h, the migrated cells were fixed, stained with crystal violet, and counted.

2.7 Western Blot Analysis

Cell lysates were prepared using RIPA buffer. Proteins (20 µg) were separated by sodium dodecyl sulfate–polyacrylamide gel electrophoresis, transferred to polyvinylidene fluoride membranes, and probed with specific primary antibodies (Table 1), followed by horseradish peroxidase–conjugated secondary antibodies. The signals were detected by enhanced chemiluminescence and quantified with ImageJ (version 1.52, National Institutes of Health, Bethesda, MD, USA).

2.8 Co-Immunoprecipitation

HPASMC lysates (500 µg) from hypoxic cells were incubated with anti-NDRG2 antibody overnight, followed by incubation with Protein A/G beads. The immunocomplexes were washed, eluted, and analyzed by Western blotting. Control immunoglobulin G was used to confirm specificity.

2.9 Statistical Analysis

The data were presented as mean ± standard deviation. Cell-based experiments comprised at least three independent biological replicates. The animal sample size

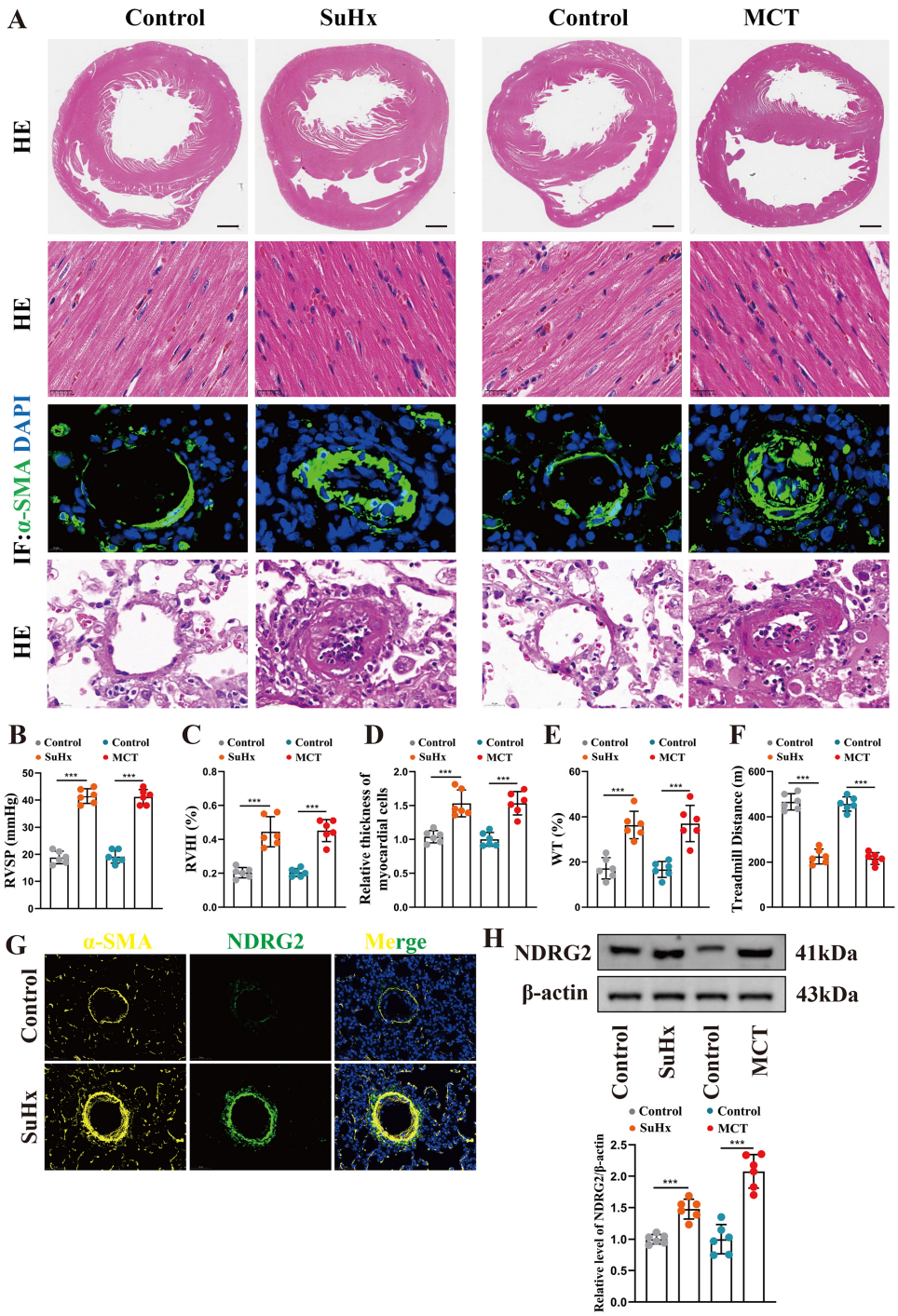

Fig. 1. NDRG2 was upregulated in experimental pulmonary hypertension rat models. (A) Representative images of heart and lung tissues from the indicated groups. Top row: Whole-heart gross morphology. Second row: H&E staining of cardiomyocytes. Third row: Immunofluorescence staining of pulmonary vessels for α-SMA (red) and NDRG2 (green). Bottom row: H&E staining of pulmonary arterioles. Scale bars: 2 mm (whole heart), 25 µm (cardiomyocytes), 10 µm (pulmonary vessels, immunofluorescence), and 20 µm (pulmonary vessels, H&E). (B–F) Quantification of RVSP (B), RVHI (C), cardiomyocyte diameter (D), arteriolar wall thickness (%) (E), and treadmill running distance (F) for each group (n = 6). (G) Representative immunofluorescence images showing co-localization of NDRG2 (green) and α-smooth muscle actin (α-SMA, red) in lung tissues from control and SuHx groups. Nuclei were counterstained with DAPI (blue). Scale bar, 50 µm. (H) Representative Western blot bands and quantitative analysis of NDRG2 protein expression in the isolated medial smooth muscle layer of pulmonary arteries from each group. $^{***}p < 0.001$. (unpaired two-tailed Student's t-test). NDRG2, N-myc downstream-regulated gene 2; H&E, Hematoxylin and eosin; α-SMA, α-smooth muscle actin; RVSP, RV systolic pressure; RVHI, RV hypertrophy index.

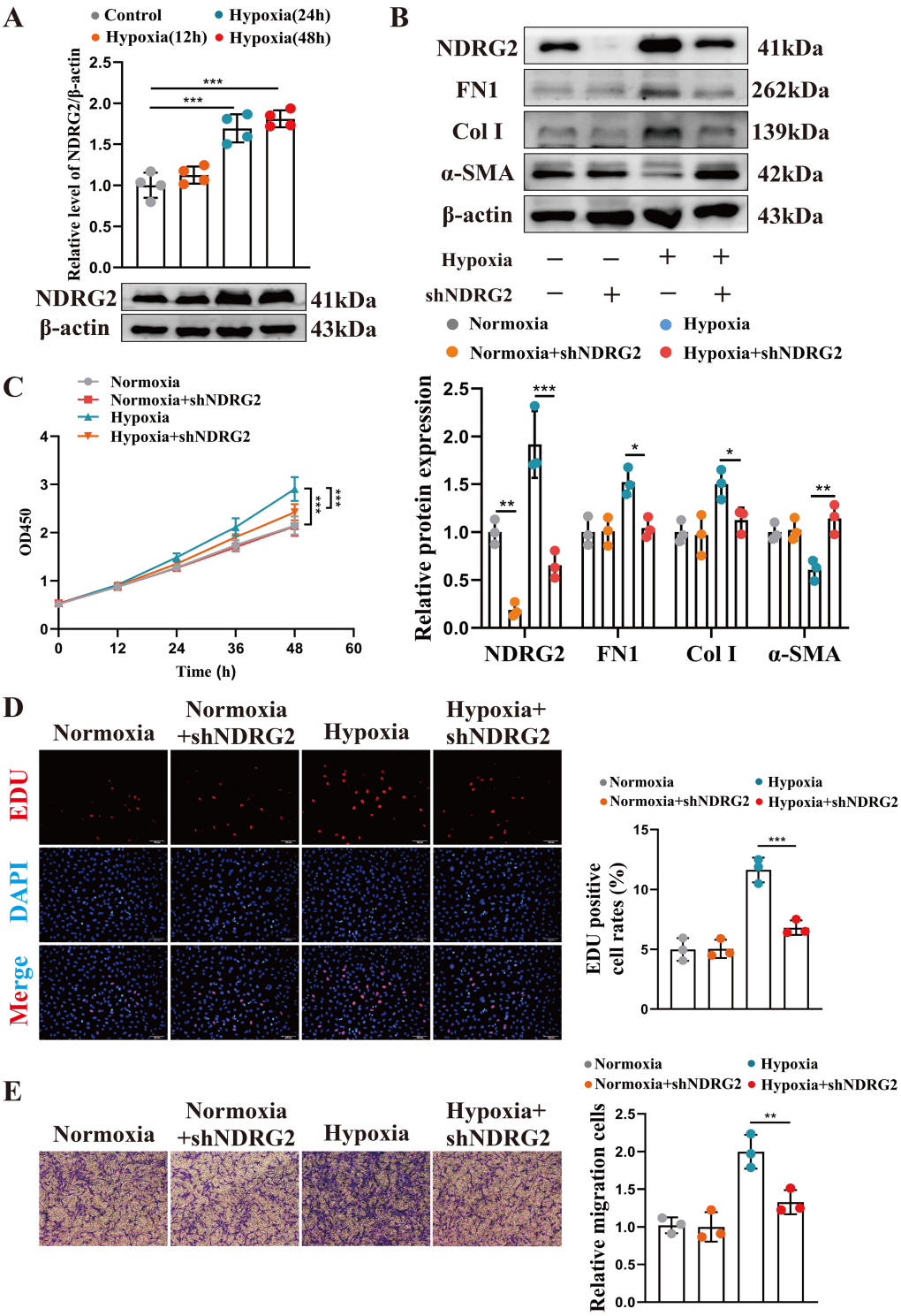

Fig. 2. NDRG2 knockdown attenuated key pathological phenotypes in hypoxic HPASMCs. (A) Western blot analysis of NDRG2 protein expression in HPASMCs exposed to hypoxia for the indicated durations. (B) Western blot analysis of NDRG2, FN1, Col I, and α-SMA under the indicated conditions. (C) Cell proliferation measured using CCK-8 assay (n = 6). (D) Proliferation assessed using EdU staining (red; nuclei blue). Scale bar, 100 µm. (E) Cell migration evaluated using the Transwell assay (crystal violet stain). Scale bar, 50 µm. $^{*}p < 0.05$, $^{**}p < 0.01$, $^{***}p < 0.001$. (one-way ANOVA with Tukey's test). HPASMCs, Human pulmonary arterial smooth muscle cells; FN1, fibronectin 1; Col I, Collagen I; CCK-8, cell counting kit-8; EdU, 5-ethynyl-2′-deoxyuridine; ANOVA, analysis of variance.

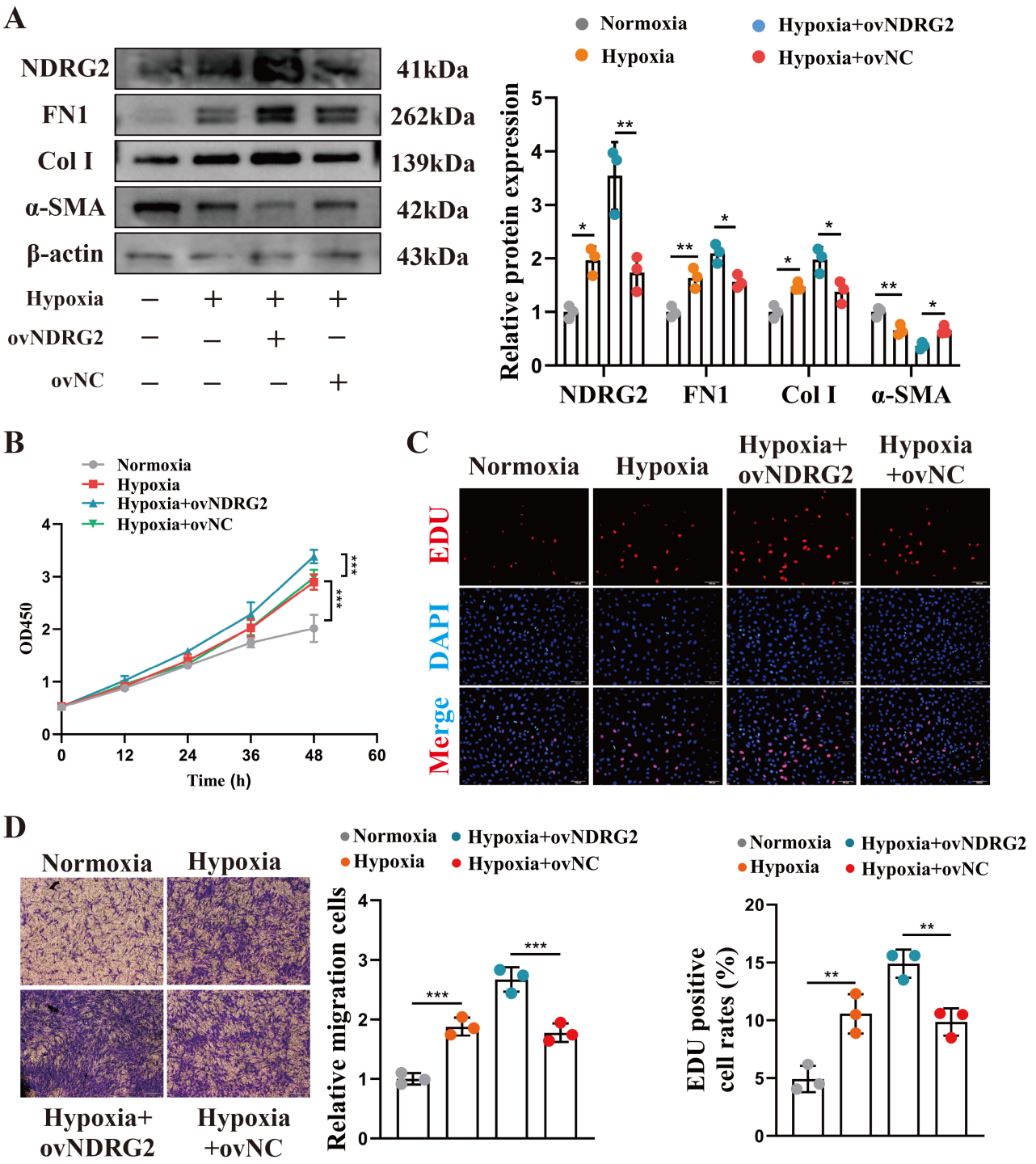

Fig. 3. NDRG2 overexpression exacerbated key pathological phenotypes in hypoxic HPASMCs. (A) Western blot analysis under indicated conditions. (B) Proliferation detected using CCK-8 assay (n = 6). (C) Proliferation by EdU staining (red). Scale bar, 100 μm. (D) Migration detected using the Transwell assay. Scale bar, 50 μm. (one-way ANOVA with Tukey's test). $^{*}p < 0.05$, $^{**}p < 0.01$, $^{***}p < 0.001$.

(n = 6 per group) was determined by power analysis (α = 0.05, β = 0.20). For each individual dataset, the normality was assessed using the Shapiro–Wilk test. For normally distributed data, two-group comparisons were made using an unpaired two-tailed Student t test, and multiple comparisons using one-way analysis of variance with Tukey's post hoc test. The nonparametric data were analyzed using the Mann–Whitney U test (two groups) or the Kruskal–Wallis

test with Dunn's correction (multiple groups). A p value less than 0.05 indicated a statistically significant difference. All analyses were performed using GraphPad Prism 9.0 (GraphPad Software, Boston, MA, USA).

3. Results

3.1 NDRG2 was Upregulated in Pulmonary Arterial Smooth Muscle in Experimental Rats With Pulmonary Hypertension

We established two widely used rat models to investigate the role of NDRG2 in PH: the SuHx model and the monocrotaline (MCT)-induced model. The model rats developed the hallmark features of PH, including significant right ventricular hypertrophy, cardiomyocyte enlargement, and pronounced pulmonary vascular remodeling and occlusion (Fig. 1A,D,E). These pathological changes were accompanied by elevated RVSP and RVHI (Fig. 1B,C), as well as impaired exercise tolerance (Fig. 1F), confirming successful establishment of the model.

Immunofluorescence staining revealed robust co-localization of NDRG2 with the smooth muscle marker α-smooth muscle actin (α-SMA) in the pulmonary vascular wall, with signal intensity markedly increased in SuHx rats (Fig. 1G). Consistent with this, Western blot analysis of isolated pulmonary arterial medial layers demonstrated a significant upregulation of NDRG2 protein in both SuHx and MCT models compared with controls (Fig. 1H). We analyzed publicly available transcriptomic data from patients with PH to assess the translational relevance of our findings. In the dataset GSE221511 [23], NDRG2 mRNA expression was significantly upregulated in PASMCs isolated from patients with thromboembolic PH compared with cells from normal controls ($p < 0.05$). This observation aligned with our results from rodent models and supported the potential clinical relevance of NDRG2 upregulation in human PH pathophysiology.

3.2 NDRG2 Drove Hypoxia-Induced Phenotypic Modulation, Proliferation, and Migration of Pulmonary Arterial Smooth Muscle Cells

We next elucidated the functional role of NDRG2 in HPASMCs. Hypoxia treatment led to a time-dependent increase in NDRG2 expression, which peaked at 24 h (Fig. 2A); this time point was thus used for subsequent experiments.

The knockdown of NDRG2 with specific shRNA (Fig. 2B) attenuated hypoxia-induced phenotypic switching from a contractile to a synthetic secretory phenotype (Fig. 2B), and suppressed cell proliferation (Fig. 2C,D) and migration (Fig. 2E). On the contrary, NDRG2 overexpression under hypoxia (Fig. 3A) exacerbated phenotypic switching (Fig. 3A), potentiated proliferation (Fig. 3B,C), and enhanced migration (Fig. 3D). These data establish NDRG2 as a key driver of pathological HPASMC behavior under hypoxic conditions.

3.3 NDRG2 Bound to DRP1 to Promote Pathogenic Mitochondrial Fission

As hypoxia disrupts cellular metabolism, we assessed the impact of NDRG2 on bioenergetics. Hypoxia reduced adenosine triphosphate (ATP) generation and increased reactive oxygen species (ROS) production in HPASMCs, both of which were rescued by NDRG2 knockdown (Fig. 4A,B).

Given the central role of mitochondria in energy production, we examined mitochondrial morphology. Staining for the mitochondrial marker TOM20 revealed that hypoxia induced extensive mitochondrial fragmentation, which was prevented by NDRG2 depletion (Fig. 4C). Although NDRG2 knockdown did not alter the total protein levels of key mitochondrial dynamics regulators (MFN1, MFN2, OPA1, and DRP1) (Fig. 4D), Co-IP using an anti-NDRG2 antibody confirmed an interaction between NDRG2 and DRP1 (Fig. 4E), which was further supported by their strong subcellular co-localization (Fig. 4F).

We then investigated DRP1 activation. Hypoxia promoted the phosphorylation of DRP1 at the Ser616 activation site and suppressed phosphorylation at the inhibitory Ser637 site. NDRG2 knockdown specifically abrogated hypoxia-induced DRP1 Ser616 phosphorylation without impacting Ser637 (Fig. 4G). Since Ser616 phosphorylation facilitates DRP1 translocation to mitochondria, we assessed this event and found that hypoxia-enhanced mitochondrial localization of DRP1 was markedly reduced upon NDRG2 knockdown (Fig. 4H). These results demonstrated that NDRG2 interacted with DRP1 and specifically promoted its phosphorylation at the Ser616 activation site under hypoxia. The specific upstream kinase responsible for this effect remains to be identified. However, the aforementioned findings establish NDRG2 as a key regulator of DRP1 activation in this setting.

3.4 NDRG2 Regulated Smooth Muscle Cell Pathology Through DRP1

We performed rescue experiments to definitively establish DRP1 as the key downstream effector of NDRG2. The knockdown of DRP1 (Fig. 5A) reversed the exacerbating effects of NDRG2 overexpression on phenotypic switching (Fig. 5A), proliferation (Fig. 5B,C), and migration (Fig. 5D) under hypoxia. These results demonstrated that NDRG2 drove HPASMC dysfunction primarily in a DRP1-dependent manner.

3.5 In Vivo Knockdown of NDRG2 Ameliorated Experimental Pulmonary Hypertension

Finally, we assessed the preventive potential of targeting NDRG2 *in vivo*. Rats received intratracheal AAV9-shNDRG2 to knock down lung NDRG2 expression 2 weeks before initiation of SuHx treatment, allowing evaluation of whether NDRG2 inhibition could attenuate disease development. The intratracheal delivery of AAV9-

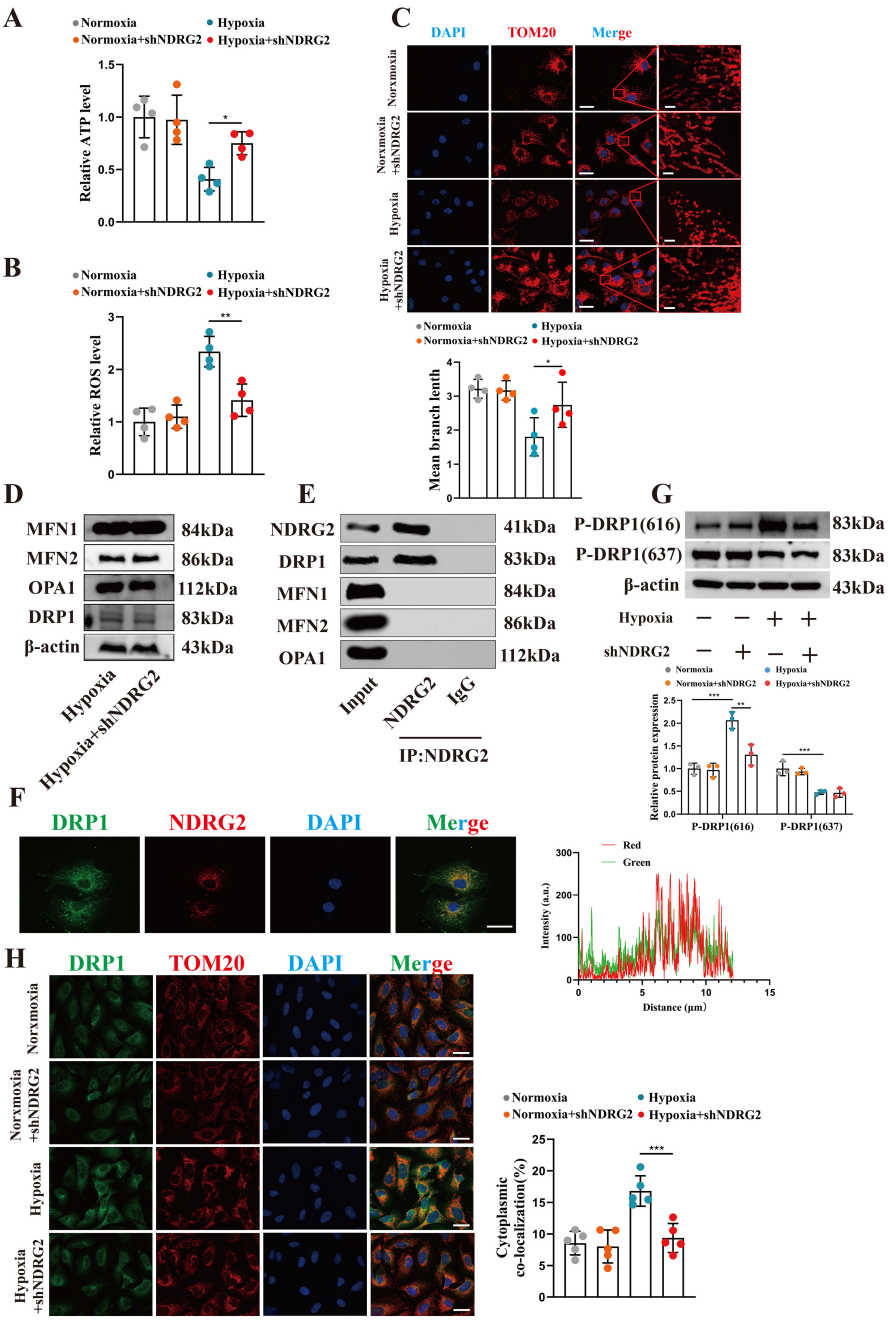

Fig. 4. NDRG2 drove mitochondrial fission by binding to and promoting the phosphorylation of DRP1. (A,B) Quantitative detection of intracellular ATP levels (A) and ROS levels (B) in HPASMCs under different treatment conditions. (C) Upper panel: Representative images of mitochondrial morphology in HPASMCs under different conditions, observed by immunofluorescence staining of TOM20. Scale bar, 10 μm. Lower panel: Quantitative analysis of mitochondrial branch length in the corresponding groups. (D) Western blot analysis of mitochondrial dynamics–related proteins (MFN1, MFN2, OPA1, and DRP1) in HPASMCs after NDRG2 knockdown. (E) Interaction between NDRG2 and DRP1 detected by co-immunoprecipitation (Co-IP) of NDRG2 from HPASMC lysates. (F) Representative immunofluorescence images and quantitative co-localization analysis of NDRG2 (red) and DRP1 (green) in hypoxic HPASMCs. Scale bar, 10 μm. (G) Representative Western blot bands and quantitative analysis of DRP1 phosphorylation levels at Ser616 and Ser637 in HPASMCs under different conditions. (H) Representative images of DRP1 mitochondrial translocation observed by co-staining of DRP1 (green) and TOM20 (red) under different conditions. Scale bar, 10 μm. $^{*}p < 0.05$, $^{**}p < 0.01$, $^{***}p < 0.001$. (unpaired two-tailed Student's *t*-test, one-way ANOVA with Tukey's test). DRP1, dynamin-related protein 1; ATP, adenosine triphosphate; ROS, reactive oxygen species; TOM20, translocase of outer membrane 20; MFN1, Mitofusin 1; OPA1, OPA1 mitochondrial dynamin like GTPase.

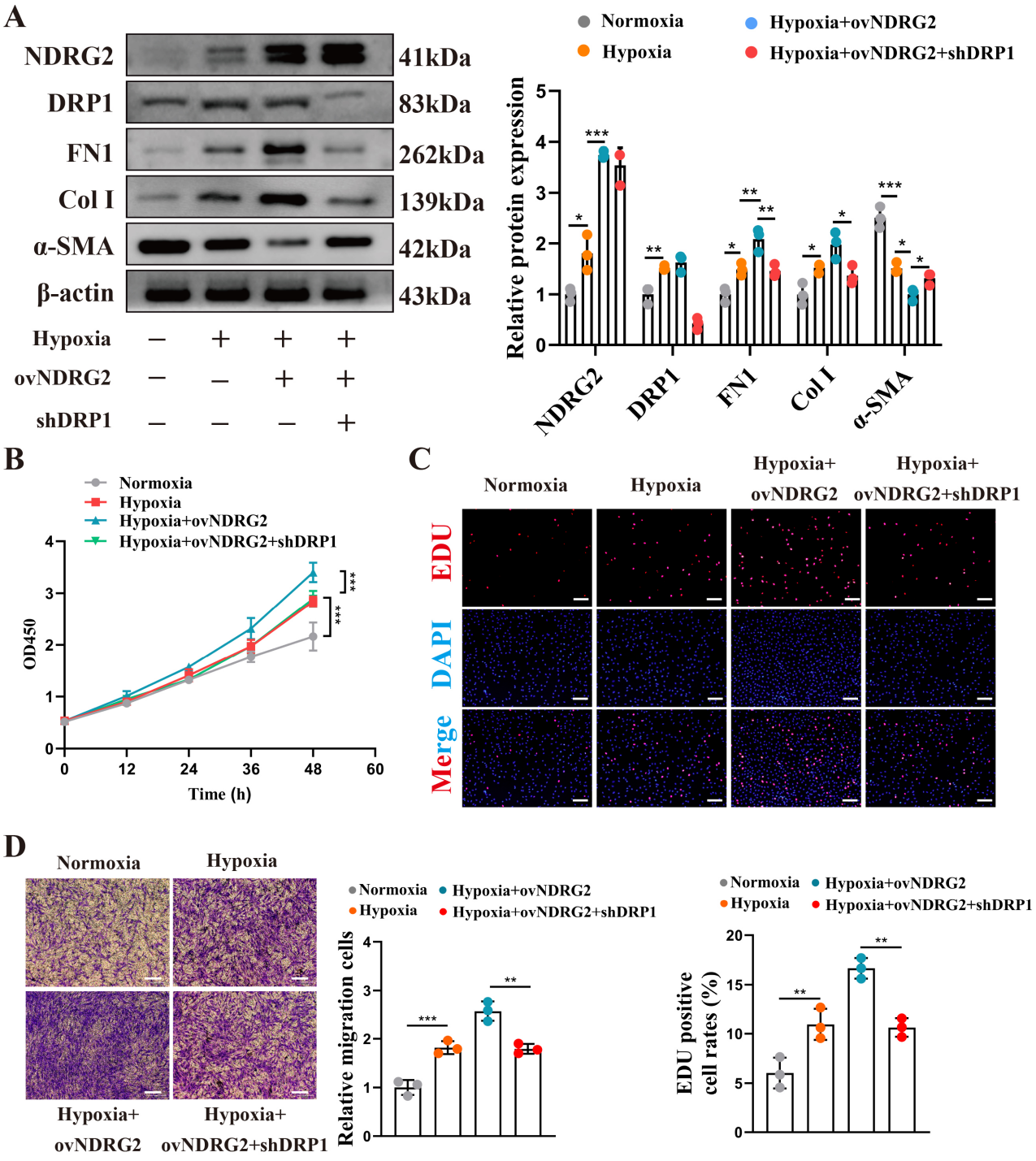

Fig. 5. NDRG2 mediated hypoxia-induced pathological behaviors in pulmonary arterial smooth muscle cells through a DRP1-dependent mechanism. (A) Western blot analysis under the indicated conditions. (B) Proliferation detected using CCK-8 assay ($n = 6$). (C) Proliferation detected using EdU staining (red). Scale bar, 200 μm. (D) Migration detected using the Transwell assay. Scale bar, 50 μm. $^{*}p < 0.05$, $^{**}p < 0.01$, $^{***}p < 0.001$. (one-way ANOVA with Tukey's test).

shNDRG2 efficiently knocked down NDRG2 expression in the lungs of SuHx rats (Fig. 6A,H). This intervention markedly attenuated disease progression, as evidenced by reduced right ventricular hypertrophy (Fig. 6B), inhibition of pulmonary vascular remodeling (Fig. 6D,E,F), and lower RVSP (Fig. 6C). Consequently, the exercise capacity of treated rats was significantly improved (Fig. 6G). Furthermore, NDRG2 knockdown reversed the pathological phenotypic switching of smooth muscle cells in isolated pulmonary arteries (Fig. 6H).

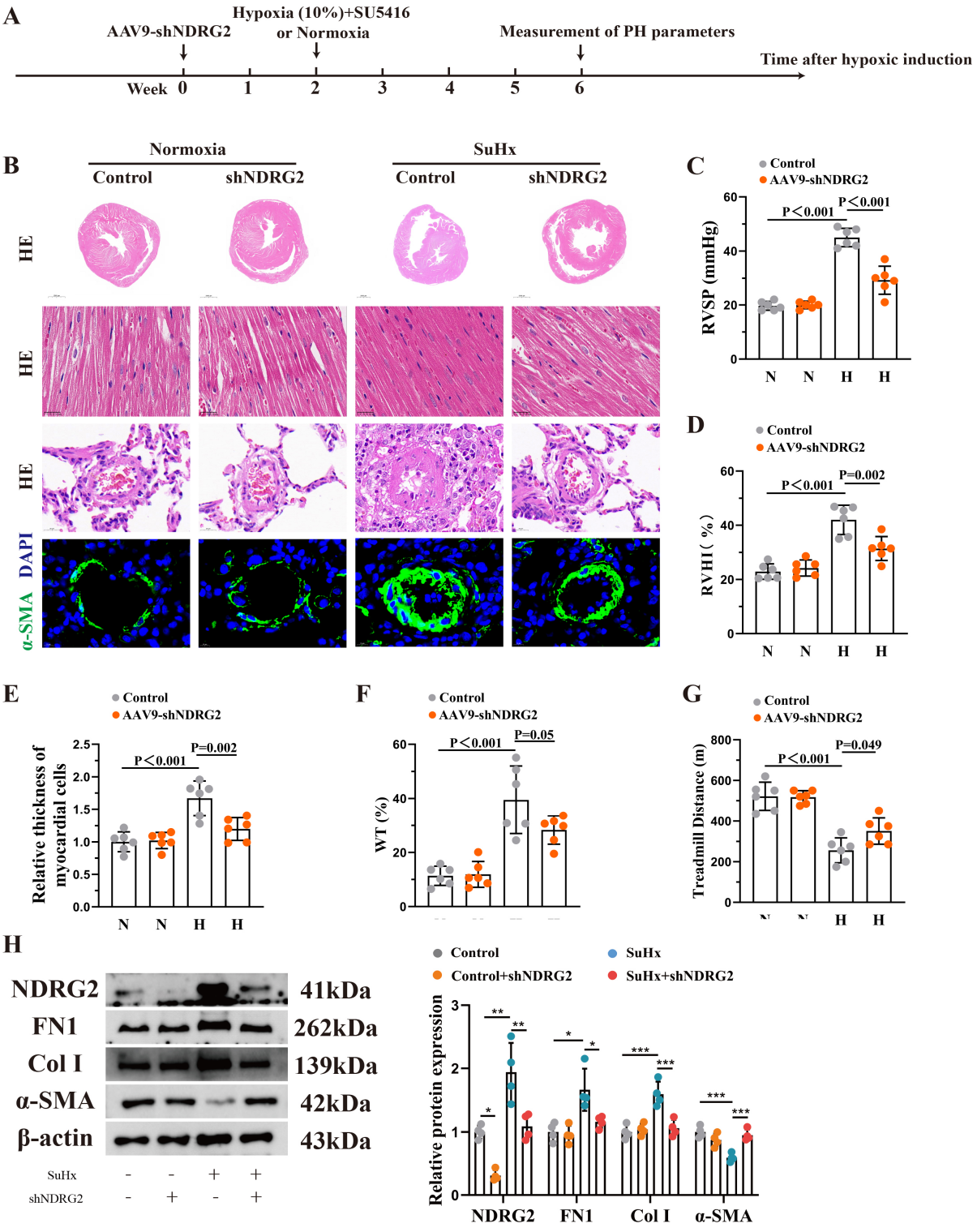

Fig. 6. *In vivo* knockdown of NDRG2 alleviated the progression of pulmonary hypertension in rats. (A) Schematic diagram of the animal experimental design. (B) Representative images of heart and lung tissue sections from the indicated groups (control, control + AAV9-shNDRG2, SuHx, and SuHx + AAV9-shNDRG2). Scale bars from top to bottom: 2 mm, 25 μm, 20 μm, and 10 μm. (C–G) Quantification of RVSP (C), RVHI (D), cardiomyocyte diameter (E), arteriolar wall thickness (%) (F), and running distance (G) ($n = 6$). (H) Western blot analysis of protein expression in isolated pulmonary arterial media. $^{*}p < 0.05$, $^{**}p < 0.01$, $^{***}p < 0.001$. (one-way ANOVA with Tukey's test). AAV9, adeno-associated virus 9.

4. Discussion

Our study identified NDRG2 as an additional member of the NDRG family involved in pulmonary vascular remodeling in PH, demonstrating its crucial role in regulating mitochondrial dynamics. We established that NDRG2 acted as a molecular switch in pathological PASMCs, linking hypoxic stress to mitochondrial fission and metabolic dysregulation through direct interaction with DRP1 and precise modulation of its phosphorylation status. This pathway ultimately drove disease progression. Our findings not only provide novel insights into PH pathogenesis but also reveal a potential therapeutic target.

The biological functions of NDRG2 are highly context dependent, varying by cell type and pathological setting, with reported roles spanning from cytoprotection to disease promotion [24,25]. This functional diversity is reflected in its variable response to hypoxia across various cell lineages, thereby underscoring the complexity of its regulation [26]. Our data definitively showed that NDRG2 is upregulated and exerts a net pro-pathogenic effect in hypoxic PASMCs, aligning with its characterization as a stress-responsive gene. Notably, our previous work identified a pro-remodeling function for its homolog NDRG1 in PH [12]. The congruent pathogenic role of NDRG2 highlighted in this study points to a conserved importance of the NDRG protein family in pulmonary vascular pathology. A comparative analysis suggests that both NDRG1 and NDRG2 may converge on disrupting mitochondrial homeostasis; however, NDRG1 has also been implicated in modulating additional pathways such as PI3K–Akt signaling. This indicates a shared nodal role in metabolic dysregulation, alongside isoform-specific mechanisms that may collectively drive vascular remodeling. Furthermore, our *in vitro* studies employed a sustained 1% O_2 exposure to robustly elicit cellular responses. In human PH, vascular cells may experience more moderate or intermittent hypoxia. Future studies investigating the threshold and dynamics of NDRG2 induction and DRP1 activation across a range of oxygen tensions may be valuable to better understand how this pathway engages across the spectrum of hypoxic stress relevant to clinical disease.

The central mechanistic advance of our work is the delineation of the NDRG2–DRP1–mitochondrial fission axis. Mitochondrial fragmentation is a well-established driver of PH pathogenesis [27,28], facilitating vascular remodeling by promoting PASMC proliferation and conferring resistance to apoptosis [17,29]. DRP1 serves as the master regulator of mitochondrial fission, with its activity predominantly controlled by opposing post-translational modifications: activating phosphorylation at Ser616 and inhibitory phosphorylation at Ser637 [16,30]. We found that NDRG2 specifically enhanced DRP1 phosphorylation at the Ser616 activation site via a direct molecular interaction, without altering total DRP1 levels or the phosphorylation status at Ser637. This selective effect suggests that NDRG2 interfaces with upstream regulators specific to the Ser616 pathway (e.g., ERK1/2 or CDK1), thereby shifting the phosphorylation balance decisively toward activation to drive pathological fission. This modification is crucial for DRP1 activation and its subsequent translocation to mitochondria. Consequently, we placed NDRG2 at a pivotal regulatory node, directly governing the DRP1 activation switch to transduce extracellular hypoxic cues into intracellular metabolic pathology, evidenced here by bioenergetic failure (reduced ATP levels) and oxidative stress (ROS accumulation). Based on this observed dysfunction, we predicted that NDRG2 overexpression also impaired mitochondrial respiratory function, leading to reduced oxygen consumption rates and compromised membrane potential. Direct measurement of these parameters in future studies can provide a more detailed resolution of the metabolic alterations downstream of the NDRG2-DRP1 axis. These pathological changes collectively propel the proliferation and migration of PASMCs.

Despite these insights, our study had certain limitations. First, our mechanistic conclusions were derived primarily from studies on PASMCs. Although this focused approach allowed detailed dissection of the NDRG2–DRP1 axis, we acknowledge that PH is a multicellular disease involving endothelial dysfunction, fibroblast activation, and immune cell infiltration. Our *in vivo* AAV9-mediated knockdown was not cell specific, and thus the therapeutic effects observed might have resulted from NDRG2 inhibition in multiple cell types. The contribution of NDRG2 within nonsmooth muscle vascular cells to PH pathogenesis remains an important area for future investigation. Second, the precise upstream mechanism whereby NDRG2 facilitates DRP1 Ser616 phosphorylation remains to be fully elucidated. Although our study established the functional consequence of this modification, identifying the responsible kinase(s) is a key remaining question. NDRG2 may act as a scaffold to recruit specific kinases known to phosphorylate DRP1 at Ser616 (e.g., ERK1/2, CDK1, or PKCδ) or may modulate the activity of counteracting phosphatases. Definitively identifying these upstream effectors using approaches such as phospho-proteomic screening or targeted genetic/pharmacologic intervention represents an essential and immediate future direction arising from this study. Third, validating NDRG2 upregulation and its correlation with disease severity in lung tissues from patients with PH may be essential to underscore the translational potential of our findings. Fourth, our *in vivo* studies were conducted exclusively in male rats. Given the established sexual dimorphism in PH incidence and progression, future investigations should include both sexes to determine the generalizability and potential sex-specific nuances of the NDRG2–DRP1 pathway. Furthermore, although our localized intratracheal delivery of AAV9-shNDRG2 aimed to minimize systemic exposure, a comprehensive assessment of potential off-target effects and the consequences of long-term

NDRG2 inhibition in other organs may be crucial considerations for future therapeutic development. Finally, from a translational perspective, our *in vivo* intervention demonstrated the preventive potential of NDRG2 inhibition when administered prior to disease induction. It is important to note that this paradigm models a preventive strategy. While the central role of the NDRG2-DRP1 axis in sustaining mitochondrial fission and PASMC dysfunction suggests that its inhibition could also ameliorate established pathology, future studies explicitly evaluating the efficacy of NDRG2-targeted therapies initiated after the full establishment of PH are needed to define their potential for disease reversal.

5. Conclusions

In summary, our study identified NDRG2 as a key upstream regulator driving pathological mitochondrial fission and vascular remodeling in PH. We demonstrated that NDRG2 was upregulated in hypoxic PASMCs and experimental PH models, where it promoted a synthetic secretory phenotype, proliferation, and migration. Mechanistically, NDRG2 directly interacted with DRP1 to specifically enhance its phosphorylation at Ser616, leading to excessive mitochondrial fission, bioenergetic dysfunction, and oxidative stress. Crucially, the genetic inhibition of NDRG2 *in vivo* ameliorated hemodynamic and structural pathologies in rats with SuHx-induced PH. These findings delineate a novel NDRG2–DRP1 axis central to PH pathogenesis in preclinical models, thereby nominating this pathway for further mechanistic and translational research (Graphical Abstract).

Availability of Data and Materials

The datasets used and analyzed in this study are available from the corresponding author upon reasonable request.

Author Contributions

JYL, JYC, YL, YSS, YYZ, YRZ, EFX, YQX, SST, HXL and WMH significantly contributed to the study, including its conception, design, execution, data acquisition, analysis, and interpretation. JYL, JYC, YL, YSS, YYZ, YRZ, EFX, YQX, SST, HXL and WMH were also involved in drafting, revising, or critically reviewing the manuscript; All authors approved the final version for publication; agreed on the journal for manuscript submission; and accepted accountability for all aspects of the study. JYL designed the study, conducted the experiments, interpreted the results, and wrote the manuscript. YSS and JYC conducted the experiments and interpreted the results. YL, YRZ and EFX contributed to the study design, conducted the experiments, and participated in manuscript revision. YYZ, YQX, SST and HXL drew icons for statistical analysis. WMH provided financial support.

Ethics Approval and Consent to Participate

The Research Ethics Committee at Ningbo University granted approval for all animal experiments and methodologies (AEWC-NBU20250371). All procedures were performed in accordance with the NIH Guide for the Care and Use of Laboratory Animals. The Laboratory Animal Science Department facilitated the procurement of Sprague–Dawley rats. Strict compliance with the established protocols for the care and use of laboratory animals was maintained throughout all experimental processes.

Acknowledgment

The authors would like to express their gratitude to all those who helped them in writing this manuscript. They thank all the peer reviewers for their opinions and suggestions.

Funding

This work was financially supported by the National Natural Science Foundation of China (Grant No. 82500082). Additional support was provided by the One Health Interdisciplinary Research Project at the Institute of One Health Science, Ningbo University, the project "Establishment of the Coronary Heart Disease Interventional Diagnosis and Treatment Center at the Cixi Integrated Traditional Chinese and Western Medicine Medical Health Group" (Grant No. 812410050), and the project "The Role of Leukocyte-Derived Chemokine 2 in Regulating Macrophage Polarization" (Grant No. 882500370).

Conflict of Interest

The authors declare no conflict of interest.

Declaration of AI and AI-Assisted Technologies in the Writing Process

During the preparation of this work the authors used DeepSeek in order to write and polish manuscripts. After using this tool/service, the authors reviewed and edited the content as needed and takes full responsibility for the content of the published article.

References

[1] Adu-Amankwaah J, Shi Y, Song H, Ma Y, Liu J, Wang H, *et al*. Signaling pathways and targeted therapy for pulmonary hypertension. Signal Transduction and Targeted Therapy. 2025; 10: 207. https://doi.org/10.1038/s41392-025-02287-8.

[2] Mocumbi A, Humbert M, Saxena A, Jing ZC, Sliwa K, Thienemann F, *et al*. Pulmonary hypertension. Nature Reviews. Disease Primers. 2024; 10: 1. https://doi.org/10.1038/s41572-023-00486-7.

[3] Kovacs G, Bartolome S, Denton CP, Gatzoulis MA, Gu S, Khanna D, *et al*. Definition, classification and diagnosis of pulmonary hypertension. The European Respiratory Journal. 2024; 64: 2401324. https://doi.org/10.1183/13993003.01324-2024.

[4] Chin KM, Gaine SP, Gerges C, Jing ZC, Mathai SC, Tamura Y, *et al*. Treatment algorithm for pulmonary arterial hypertension.

The European Respiratory Journal. 2024; 64: 2401325. https://doi.org/10.1183/13993003.01325-2024.

[5] Vonk Noordegraaf A, Chin KM, Haddad F, Hassoun PM, Hemnes AR, Hopkins SR, *et al*. Pathophysiology of the right ventricle and of the pulmonary circulation in pulmonary hypertension: an update. The European Respiratory Journal. 2019; 53: 1801900. https://doi.org/10.1183/13993003.01900-2018.

[6] Thenappan T, Ormiston ML, Ryan JJ, Archer SL. Pulmonary arterial hypertension: pathogenesis and clinical management. BMJ (Clinical Research Ed.). 2018; 360: j5492. https://doi.org/10.1136/bmj.j5492.

[7] Olsson KM, Corte TJ, Kamp JC, Montani D, Nathan SD, Neubert L, *et al*. Pulmonary hypertension associated with lung disease: new insights into pathomechanisms, diagnosis, and management. The Lancet. Respiratory Medicine. 2023; 11: 820–835. https://doi.org/10.1016/S2213-2600(23)00259-X.

[8] Feng D, Zhou J, Liu H, Wu X, Li F, Zhao J, *et al*. Astrocytic NDRG2-PPM1A interaction exacerbates blood-brain barrier disruption after subarachnoid hemorrhage. Science Advances. 2022; 8: eabq2423. https://doi.org/10.1126/sciadv.abq2423.

[9] Yao L, Zhang J, Liu X. NDRG2: a Myc-repressed gene involved in cancer and cell stress. Acta Biochimica et Biophysica Sinica. 2008; 40: 625–635. https://doi.org/10.1111/j.1745-7270.2008.00434.x.

[10] Wang L, Liu N, Yao L, Li F, Zhang J, Deng Y, *et al*. NDRG2 is a new HIF-1 target gene necessary for hypoxia-induced apoptosis in A549 cells. Cellular Physiology and Biochemistry: International Journal of Experimental Cellular Physiology, Biochemistry, and Pharmacology. 2008; 21: 239–250. https://doi.org/10.1159/000113765.

[11] Su ZH, Liao HH, Lu KE, Chi Z, Qiu ZQ, Jiang JM, *et al*. Hypoxia-responsive miR-346 promotes proliferation, migration, and invasion of renal cell carcinoma cells via targeting NDRG2. Neoplasma. 2020; 67: 1002–1011. https://doi.org/10.4149/neo_2020_190917N915.

[12] Liu Y, Luo Y, Shi X, Lu Y, Li H, Fu G, *et al*. Role of KLF4/NDRG1/DRP1 axis in hypoxia-induced pulmonary hypertension. Biochimica et Biophysica Acta. Molecular Basis of Disease. 2023; 1869: 166794. https://doi.org/10.1016/j.bbadis.2023.166794.

[13] Sun Z, Tong G, Ma N, Li J, Li X, Li S, *et al*. NDRG2: a newly identified mediator of insulin cardioprotection against myocardial ischemia-reperfusion injury. Basic Research in Cardiology. 2013; 108: 341. https://doi.org/10.1007/s00395-013-0341-5.

[14] Sun Z, Shen L, Sun X, Tong G, Sun D, Han T, *et al*. Variation of NDRG2 and c-Myc expression in rat heart during the acute stage of ischemia/reperfusion injury. Histochemistry and Cell Biology. 2011; 135: 27–35. https://doi.org/10.1007/s00418-010-0776-9.

[15] Zhao J, Zhao Q, Mao S. N-myc downstream regulated gene 2 ameliorates myocardial remodeling and cardiac function in heart failure rats. Human & Experimental Toxicology. 2021; 40: 1296–1307. https://doi.org/10.1177/0960327121993208.

[16] Jin JY, Wei XX, Zhi XL, Wang XH, Meng D. Drp1-dependent mitochondrial fission in cardiovascular disease. Acta Pharmacologica Sinica. 2021; 42: 655–664. https://doi.org/10.1038/s41401-020-00518-y.

[17] Breault NM, Wu D, Dasgupta A, Chen KH, Archer SL. Acquired disorders of mitochondrial metabolism and dynamics in pulmonary arterial hypertension. Frontiers in Cell and Developmental Biology. 2023; 11: 1105565. https://doi.org/10.3389/fcell.2023.1105565.

[18] Riou M, Enache I, Sauer F, Charles AL, Geny B. Targeting Mitochondrial Metabolic Dysfunction in Pulmonary Hypertension: Toward New Therapeutic Approaches? International Journal of Molecular Sciences. 2023; 24: 9572. https://doi.org/10.3390/ijms24119572.

[19] Feng W, Wang J, Yan X, Zhang Q, Chai L, Wang Q, *et al*. ERK/Drp1-dependent mitochondrial fission contributes to HMGB1-induced autophagy in pulmonary arterial hypertension. Cell Proliferation. 2021; 54: e13048. https://doi.org/10.1111/cpr.13048.

[20] Deng X, Que Q, Zhang K, Li B, Yang N, Hu Q, *et al*. Mechanistic insights into the role of EGLN3 in pulmonary vascular remodeling and endothelial dysfunction. Respiratory Research. 2025; 26: 61. https://doi.org/10.1186/s12931-025-03144-6.

[21] Deng X, Qiu P, Li X, Hu Y, Que Q, Zhang K, *et al*. Potential of Sivelestat for Pulmonary Arterial Hypertension Treatment: Network Pharmacology-Based Target Identification and Mechanistic Exploration. Drug Design, Development and Therapy. 2025; 19: 4123–4138. https://doi.org/10.2147/DDDT.S507240.

[22] Liu Y, Deng X, He C, Lv S, Que Q, Li B, *et al*. NDRG1-HIF1α interaction in hypoxic signaling for pulmonary hypertension. International Journal of Biological Macromolecules. 2026; 339: 149857. https://doi.org/10.1016/j.ijbiomac.2025.149857.

[23] Kuramoto K, Ogawa A, Kiyama K, Matsubara H, Ohno Y, Fuchikami C, *et al*. Antiproliferative effect of selexipag active metabolite MRE-269 on pulmonary arterial smooth muscle cells from patients with chronic thromboembolic pulmonary hypertension. Pulmonary Circulation. 2023; 13: e12231. https://doi.org/10.1002/pul2.12231.

[24] Park KC, Paluncic J, Kovacevic Z, Richardson DR. Pharmacological targeting and the diverse functions of the metastasis suppressor, NDRG1, in cancer. Free Radical Biology & Medicine. 2020; 157: 154-175. https://doi.org/10.1016/j.freeradbiomed.2019.05.020.

[25] Lee KW, Lim S, Kim KD. The Function of N-Myc Downstream-Regulated Gene 2 (NDRG2) as a Negative Regulator in Tumor Cell Metastasis. International Journal of Molecular Sciences. 2022; 23: 9365. https://doi.org/10.3390/ijms23169365.

[26] Tsui KH, Hou CP, Chang KS, Lin YH, Feng TH, Chen CC, *et al*. Metallothionein 3 Is a Hypoxia-Upregulated Oncogene Enhancing Cell Invasion and Tumorigenesis in Human Bladder Carcinoma Cells. International Journal of Molecular Sciences. 2019; 20: 980. https://doi.org/10.3390/ijms20040980.

[27] Pokharel MD, Garcia-Flores A, Marciano D, Franco MC, Fineman JR, Aggarwal S, *et al*. Mitochondrial network dynamics in pulmonary disease: Bridging the gap between inflammation, oxidative stress, and bioenergetics. Redox Biology. 2024; 70: 103049. https://doi.org/10.1016/j.redox.2024.103049.

[28] Ryan J, Dasgupta A, Huston J, Chen KH, Archer SL. Mitochondrial dynamics in pulmonary arterial hypertension. Journal of Molecular Medicine (Berlin, Germany). 2015; 93: 229–242. https://doi.org/10.1007/s00109-015-1263-5.

[29] Pan Z, Yao Y, Liu X, Wang Y, Zhang X, Zha S, *et al*. Nr1d1 inhibition mitigates intermittent hypoxia-induced pulmonary hypertension via Dusp1-mediated Erk1/2 deactivation and mitochondrial fission attenuation. Cell Death Discovery. 2024; 10: 459. https://doi.org/10.1038/s41420-024-02219-5.

[30] Xu C, Wang B, Li M, Dong Z, Chen N, Duan J, *et al*. FUNDC1/USP15/Drp1 ameliorated TNF-α-induced pulmonary artery endothelial cell proliferation by regulating mitochondrial dynamics. Cellular Signalling. 2024; 113: 110939. https://doi.org/10.1016/j.cellsig.2023.110939.